Metanx Alleviates Multiple Manifestations of Peripheral Neuropathy and Increases Intraepidermal Nerve Fiber Density in Zucker Diabetic Fatty Rats

Hanna Shevalye, Pierre Watcho, Roman Stavniichuk, Elena Dyukova, Sergey Lupachyk, and Irina G. Obrosova

Metanx is a product containing L-methylfolate, pyridoxal 5′-phosphate, and methylcobalamin for management of endothelial dysfunction. Metanx ingredients counteract endothelial nitric oxide synthase uncoupling and oxidative stress in vascular endothelium and peripheral nerve. This study evaluates Metanx on diabetic peripheral neuropathy in ZDF rats, a model of type 2 diabetes. Metanx was administered to 15-week-old ZDF and ZDF lean rats at either 4.87 mg · kg^{-1} · day^{-1} (a body weight–based equivalent of human dose) or 24.35 mg · kg^{-1} · day^{-1} by oral gavage two times a day for 4 weeks. Both doses alleviated hind limb digital sensory, but not sciatic motor, nerve conduction slowing and thermal and mechanical hypoalgesia in the absence of any reduction of hyperglycemia. Low-dose Metanx increased intraepidermal nerve fiber density but did not prevent morphometric changes in distal tibial nerve myelinated fibers. Metanx treatment counteracted endothelial nitric oxide synthase uncoupling, inducible nitric oxide synthase upregulation, and methylglyoxal-derived advanced glycation end product, nitrotyrosine, and nitrite/nitrate accumulation in the peripheral nerve. In conclusion, Metanx, at a body weight–based equivalent of human dose, increased intraepidermal nerve fiber density and improved multiple parameters of peripheral nerve function in ZDF rats. Clinical studies are needed to determine if Metanx finds use in management of diabetic peripheral neuropathy. ***Diabetes*** **61:2126–2133, 2012**

Diabetic peripheral neuropathy (DPN) affects at least 50% of patients with type 1 and type 2 diabetes and is a leading cause of foot amputation (1). Clinical indications of DPN include increased vibration and thermal perception thresholds that progress to sensory loss, occurring in conjunction with degeneration of all fiber types in peripheral nerve. A proportion of patients with DPN also describe abnormal sensations such as paresthesias, allodynia, hyperalgesia, and spontaneous pain that sometimes coexist with loss of normal sensory function. Several studies identify associations between diabetes-associated changes in microvessel function and morphology and DPN (2–4). In particular, in the Rochester Diabetic Neuropathy Study in patients with both type 1 and type 2 diabetes, microvessel disease was associated with the severity of diabetic polyneuropathy (3). In the EURODIAB Prospective Complications Study in patients with type 1 diabetes, low peripheral nerve conduction velocities and amplitudes were strongly associated with other diabetic microvascular complications, such as nephropathy and retinopathy (5).

Multiple biochemical mechanisms have been implicated in the pathogenesis of DPN in animal studies (6). Oxidative-nitrosative stress manifest by accumulation of lipid peroxidation products, 4-hydroxynonenal adducts, nitrated proteins, and 8-hydroxy-2′-deoxyguanosine is present in peripheral nerve, spinal cord, and dorsal root ganglion neurons of diabetic rats and mice (6–9). Diabetes-associated formation of superoxide and nitrotyrosine was described in vasa nervorum (10,11). Although experimental studies suggest that oxidative-nitrosative stress is a key mechanism contributing to nerve blood flow and nerve conduction deficits, small sensory nerve fiber dysfunction, and morphological manifestations of DPN (6,8,9,11), the efficacy of the antioxidant α-lipoic acid in clinical neuropathy trials was modest (12,13). Note, however, that experimental studies reveal adverse metabolic effects of α-lipoic acid, such as acceleration of glucose transport and sorbitol pathway activation in peripheral nerve (14,15). Furthermore, both α-lipoic and dihydrolipoic acids can act as prooxidants, and the factors determining a fragile balance between the beneficial (antioxidant) and detrimental (prooxidant) effects of either compound are not completely understood. Finding other medications to effectively combat oxidative-nitrosative stress and DPN, especially among drugs already used in clinical practice, remains highly warranted.

Metanx is a prescription combination product containing L-methylfolate, pyridoxal 5′-phosphate, and methylcobalamin (2.8:25:2) for dietary management of endothelial dysfunction. The active metabolite of folate, L-methylfolate, stabilizes and enhances production of tetrahydrobiopterin, a cofactor of endothelial nitric oxide synthase (eNOS) (16). It counteracts eNOS uncoupling and associated superoxide generation, upregulation of inducible nitric oxide synthase (iNOS), and formation of the highly reactive oxidant peroxynitrite in vascular endothelium (17). Methylcobalamin (a coenzyme form of vitamin B12, cobalamin), which promotes myelination and transport of axonal cytoskeleton, prevented reduced glutathione (GSH) depletion in peripheral nerve of diabetic rats (18). Through the methylation cycle (19), methylcobalamin can be converted to cyanocobalamin, which reacts with superoxide at the rate approaching that of superoxide dismutase (20) and with peroxynitrite, at least an order of magnitude faster than Tyr (21). Pyridoxal phosphate, known to trap 3-deoxyglucosone, to inhibit formation of advanced glycation end products (AGEs), and to act as a metal chelator, displayed antioxidant properties in several tissue sites for diabetes complications (22). Individual ingredients

From the Pennington Biomedical Research Center, Louisiana State University System, Baton Rouge, Louisiana.
Corresponding author: Irina G. Obrosova, obrosoig@pbrc.edu.
Received 31 October 2011 and accepted 12 March 2012.
DOI: 10.2337/db11-1524
H.S. and P.W. contributed equally to this study.

of Metanx improved bioavailability of nitric oxide (NO) in type 2 diabetic subjects (L-methylfolate) (23) and alleviated paresthesias and dysesthesias in subjects with DPN (methylcobalamin) (24). On the basis of the aforementioned findings, we hypothesized that Metanx more effectively counteracts oxidative-nitrosative stress and DPN than any of its ingredients. We therefore evaluated Metanx on oxidative-nitrosative stress and manifestations of DPN in Zucker diabetic fatty (ZDF) rats, a generally accepted model of type 2 diabetes.

RESEARCH DESIGN AND METHODS

Reagents. Metanx was provided by Pan American Laboratories (Covington, LA). For immunohistochemistry, the following were obtained: rabbit polyclonal anti-protein gene product 9.5 anti-serum for assessment of intraepidermal nerve fiber density (INFD) from UltraClone (Isle of Wight, U.K.); rabbit polyclonal antibodies against eNOS and iNOS and mouse monoclonal antibody against S-100 protein from Santa Cruz Biotechnology (Santa Cruz, CA); Alexa Fluor 594–conjugated isolectin GS-IB4 (*Griffonia simplicifolia*), Alexa Fluor 594–conjugated goat anti-mouse and goat anti-rabbit IgGs, and Alexa Fluor 488 goat anti-rabbit highly cross-adsorbed IgG (H+L) from Life Technologies (Eugene, OR); rabbit polyclonal antibody against Neurofilament H from EMD Millipore (Billerica, MA); Alexa Fluor 488–conjugated AffiniPure Fab fragment goat anti-rabbit IgG from Jackson ImmunoResearch Laboratories (West Grove, PA); SuperBlock blocking buffer from Thermo Scientific (Rockford, IL); and the optimum cutting temperature compound from Sakura Finetek USA (Torrance, CA). VECTASHIELD Mounting Medium was obtained from Vector Laboratories (Burlingame, CA). Other reagents for immunohistochemistry were purchased from Dako Laboratories (Santa Barbara, CA). For Western blot analysis, rabbit polyclonal antibody against iNOS was obtained from Abcam (Cambridge, MA); rabbit polyclonal antibody against eNOS dimer and monomer was purchased from BD Transduction Laboratories (Lexington, KY); mouse monoclonal antibody against methylglyoxal-derived AGE was purchased from TransGenic (Kobe, Japan); and horseradish peroxidase–conjugated anti-mouse and anti-rabbit IgGs were obtained from Cell Signaling (Danvers, MA). All other chemicals were of reagent-grade quality and were purchased from Sigma-Aldrich Chemical Company (St. Louis, MO).

Animals. The experiments were performed in accordance with the National Institutes of Health (NIH) "Principles of Laboratory Animal Care, 1985 Revised Version" and Pennington Biomedical Research Center Protocol for Animal Studies. Male 9-week-old ZDF and ZDF lean rats were purchased from Charles River (Wilmington, MA). They were fed a Purina 5008 diet (Charles River) or standard rat chow (PMI Nutrition International, Brentwood, MO), respectively, and had access to water ad libitum. At age 15 weeks, rats were weighed, blood samples for glucose measurements were taken from the tail vein, and assessment of motor and sensory nerve conduction velocities (MNCVs and SNCVs, respectively) and small sensory nerve fiber function was performed. Then, in experiment 1, ZDF and ZDF lean rats were divided into groups maintained with or without Metanx treatment for another 4 weeks, after which nerve functional studies were performed again. Metanx was administered as an aqueous solution at either 4.87 mg $\cdot$ kg^{-1} $\cdot$ day^{-1} (a body weight–based equivalent of human dose) or 24.35 mg $\cdot$ kg^{-1} $\cdot$ day^{-1} two times a day by oral gavage. In experiment 2, 19-week-old ZDF and ZDF lean rats were used for immunohistochemical studies.

Anesthesia, killing, and tissue sampling. The animals were sedated by CO_2 and killed by cervical dislocation. In experiment 1, sciatic nerves (a portion above the bifurcation point) were immediately frozen in liquid nitrogen and stored at –80°C before nitrate/nitrite, nitrotyrosine, eNOS dimer and monomer, iNOS, methylglyoxal-derived AGE, and GSH measurements. Distal tibial nerves and footpads were fixed and processed (25) for morphometric measurements and assessment of INFD. In experiment 2, sciatic nerves of ZDF and ZDF lean rats were fixed in 4% formaldehyde and used for eNOS and iNOS localization to endothelial and Schwann cells and axons.

Nerve functional studies. Sciatic MNCVs and hind limb digital SNCVs, thermal algesia (Hargreaves method), mechanical algesia (Randall-Selitto test), and tactile response thresholds (flexible von Frey filament test) were evaluated as described (6,25).

INFD. Three longitudinal 50-μm-thick footpad sections from each rat were cut on Leica CM1950 cryostat (Leica Microsystems, Nussloch, Germany) and processed as described (25). Representative images of intraepidermal nerve fibers were obtained by confocal laser scanning microscopy at ×400 magnification using Leica TCS SP5 confocal system.

Distal tibial nerve morphometry. Nerve fiber diameter and density, axonal diameter (inner), and myelin thickness were assessed as described (25). Semithin transverse nerve sections (1 μm thick) were stained with p-phenylenediamine. Nerve fiber number was counted for each section. Nerve section area and individual nerve fiber and axonal diameters were measured at a ×1,600 magnification using NIH ImageJ software (version 1.42q), and nerve fiber density and myelin thickness were calculated.

Nitrate/nitrite and nitrotyrosine. Sciatic nerve nitrotyrosine and nitrate/nitrite concentrations were measured with the OxiSelect Nitrotyrosine ELISA kit (Cell Biolabs, San Diego, CA) and the Nitrate/Nitrite Fluorometric Assay kit (Cayman Chemical Company, Ann Arbor, MI) as described (8) and were normalized per milligram protein. FlexStation 2 scanning fluorometer (Molecular Devices Corporation, Sunnyvale, CA) was used in the nitrate/nitrite assay. Protein was measured with the bicinchoninic acid protein assay (Pierce Biotechnology, Rockford, IL).

eNOS dimer and monomer, iNOS, and methylglyoxal-derived AGE. Western blot analysis of sciatic nerve iNOS and methylglyoxal-derived AGE was performed as described (8). In eNOS analysis, a loading buffer did not contain β-mercaptoethanol, and the heating procedure was omitted (26). We used 7.5% (eNOS/iNOS) and 5–20% (methylglyoxal-derived AGE) SDS-PAGE, and the electrophoresis was conducted for 2 h. Protein bands were visualized with Western Lightning Ultra (PerkinElmer, Waltham, MA) and Amersham ECL Western Blotting Detection Reagent (Little Chalfont, Buckinghamshire, U.K.) in eNOS/iNOS and methylglyoxal-derived AGE analyses, respectively. Membranes were then stripped (8) and reprobed with antibodies against β-actin (iNOS and methylglyoxal-derived AGE) or lamin B_1 (eNOS).

GSH. Sciatic nerve GSH was measured by enzymatic spectrofluorometric assay (15).

Localization of eNOS and iNOS. Sciatic nerve sections were processed as described (8,9). For eNOS and iNOS localization to Schwann cells, anti-eNOS or -iNOS antibodies were applied in combination with anti–S-100 antibody. After incubation with primary antibodies, the sections were washed in 50 mmol/L Tris-buffered saline, pH 8.4, containing 0.3% Triton X-100. A cocktail of secondary Alexa Fluor 488–conjugated AffiniPure Fab fragment goat anti-rabbit IgG and Alexa Fluor 594–conjugated goat anti-mouse antibody was then added. For eNOS and iNOS localization to axons and endothelial cells, the sections were incubated with anti-eNOS or -iNOS antibodies, washed, and incubated again with Alexa Fluor 488–conjugated AffiniPure Fab fragment goat anti-rabbit IgG. Then the sections were incubated with antibody against Neurofilament H (localization to axons), washed, and incubated again with Alexa Fluor 594–conjugated goat anti-rabbit antibody. For localization to endothelial cells, the sections were incubated with Alexa Fluor 594–conjugated isolectin. All the sections were coverslipped and mounted with VECTASHIELD Mounting Medium. Microphotographs of stained sections were taken with a 3I Everest imaging system (Intelligent Imaging Innovations, Inc., Denver, CO) equipped with an Axioplan 2 microscope (Zeiss). To verify specificity of all immunostainings, primary antibodies were omitted in negative controls.

Statistical analysis. Results are expressed as mean ± SEs. Individual comparisons between ZDF and ZDF lean rats before treatment were made using the unpaired two-tailed Student *t* test or Mann-Whitney rank sum test where appropriate. Significance was defined at $P \leq 0.05$. For multiple group comparisons (19-week-old untreated and Metanx-treated ZDF and ZDF lean rats), data were subjected to equality of variance *F* test and then to log transformation, if necessary, before one-way ANOVA. Where overall significance ($P < 0.05$) was attained, individual between-group comparisons were made using the Student-Newman-Keuls multiple range test. Significance was defined at $P \leq 0.05$. When between-group variance differences could not be normalized by log transformation (datasets for final body weights and plasma glucose), the data were analyzed by nonparametric Kruskal-Wallis one-way ANOVA followed by Bonferroni/Dunn or Fisher protected least significant differences tests for multiple comparisons.

RESULTS

Body weights and nonfasting blood glucose concentrations were increased by 56 and 41%, respectively, in the 15-week-old ZDF rats compared with the age-matched ZDF lean rats ($P < 0.01$ for both comparisons) (Table 1). The differences in the two variables deepened for 19-week-old ZDF and ZDF lean rats. Metanx treatment did not affect weight gain in ZDF lean rats. It slightly reduced weight gain in ZDF rats, but the difference with the untreated group did not achieve statistical significance. Final nonfasting blood glucose concentrations were similar in Metanx-treated ZDF and ZDF lean rats and the corresponding untreated groups.

MNCVs were reduced by 19 and 17% in 15- and 19-week-old ZDF rats compared with the age-matched ZDF lean rat group ($P < 0.01$ for both comparisons) (Table 2). Diabetes-induced MNCV deficit was not improved by Metanx at either

TABLE 1
Body weights and blood glucose concentrations in ZDF and ZDF lean rats maintained with or without Metanx treatment

Group variable	ZDF lean	ZDF lean + M1	ZDF lean + M2	ZDF	ZDF + M1	ZDF + M2
Experiment 1						
Before treatment						
Body weight (g)	292 ± 4	291 ± 11	293 ± 5	388 ± 14**	392 ± 7**	394 ± 8**
Blood glucose (mmol/L)	6.1 ± 0.15	6.1 ± 0.15	6.0 ± 0.10	17.5 ± 2.3**	17.7 ± 2.4**	17.5 ± 2.0**
After treatment						
Body weight (g)	352 ± 6	359 ± 10	353 ± 9	555 ± 16**	519 ± 17**	521 ± 12**
Blood glucose (mmol/L)	6.3 ± 0.21	6.2 ± 0.17	6.1 ± 0.15	33.3 ± 0.6**	32.1 ± 0.8**	32.2 ± 0.6**
Experiment 2						
Body weight (g)	344 ± 7			521 ± 13**		
Blood glucose (mmol/L)	6.4 ± 0.2			30.1 ± 3.4**		

Data are means ± SEM. n = 8–13 rats per group in experiment 1; n = 6 rats per group in experiment 2. M1 and M2, Metanx at low and high doses, respectively. **$P < 0.01$ vs. age-matched ZDF lean rats.

low or high dose. SNCVs were reduced by 13 and 18% in 15- and 19-week-old ZDF rats compared with age-matched ZDF lean rats ($P < 0.01$ for both comparisons). Both low and high doses of Metanx partially reversed SNCV deficit in ZDF rats ($P < 0.05$ and $P < 0.01$ compared with the corresponding untreated group) without affecting SNCV in ZDF lean rats.

Thermal response latencies were increased by 72 and 59% in 15- and 19-week-old ZDF rats compared with ZDF lean rats ($P < 0.01$ for both comparisons), consistent with the presence of thermal hypoalgesia. This condition was alleviated, although not completely corrected, by both doses of Metanx. Neither low nor high doses of Metanx affected thermal sensitivity in ZDF lean rats.

ZDF rats displayed reduced sensitivity to mechanical noxious stimuli. Paw-pressure withdrawal thresholds were increased by 49 and 36% in 15- and 19-week-old ZDF rats compared with ZDF lean rats ($P < 0.01$ for both comparisons). Both doses of Metanx corrected mechanical hypoalgesia in ZDF rats without affecting mechanical withdrawal thresholds in ZDF lean rats.

Tactile response thresholds were reduced by 45 and 55% in 15- and 19-week-old ZDF rats compared with ZDF lean rats ($P < 0.01$ for both comparisons), consistent with the presence of tactile allodynia. Low-dose Metanx treatment did not affect tactile response thresholds in ZDF rats, whereas high-dose Metanx partially corrected tactile allodynia ($P < 0.01$ vs. untreated ZDF rats, and $P < 0.01$ vs. ZDF lean rats). Neither low nor high doses of Metanx affected tactile response thresholds in ZDF lean rats.

Because nerve functional studies show efficacy of the low-dose Metanx on SNCV deficit and small fiber–mediated sensory loss, as well as only minimal advantage (effect on tactile allodynia) of the higher dose, the morphological and biochemical measurements were performed in rats treated with the low-dose Metanx only. INFD was reduced by 26% in 15-week-old ZDF rats compared with ZDF lean rats, indicating the presence of small sensory nerve fiber degeneration (Fig. 1). During the next 4 weeks of age, INFD decreased by 4.5 and 3.6% in ZDF and ZDF lean rats, respectively. Metanx, at a body weight–based equivalent of human dose, increased INFD in diabetic rats. Intraepidermal nerve fiber loss was 41% lower in Metanx-treated ZDF rats than in either 15- or 19-week-old ZDF rats that did not receive Metanx ($P < 0.01$). Metanx did not affect INFD in ZDF lean rats.

ZDF rats aged 19 weeks manifested mild atrophic changes in distal tibial nerve myelinated fibers (Table 3). At the end of the study, distal tibial nerve fiber diameter and density as well as axon diameter were indistinguishable among 19-week-old ZDF and ZDF lean rats maintained with or without Metanx treatment. Myelin thickness was reduced by 10% in

TABLE 2
Indices of peripheral nerve function in ZDF and ZDF lean rats maintained with or without Metanx treatment

Group variable	ZDF lean	ZDF lean + M1	ZDF lean + M2	ZDF	ZDF + M1	ZDF + M2
Before treatment						
MNCV (m/s)	56.6 ± 1.1			45.9 ± 1.3**		
SNCV (m/s)	43.5 ± 0.6			37.8 ± 0.6**		
Thermal response latency (s)	10.2 ± 0.3			17.5 ± 0.6**		
Mechanical withdrawal thresholds (g)	88 ± 3.4			131 ± 4.9**		
Tactile response thresholds (g)	14.1 ± 1.4			8.0 ± 1.1**		
After treatment						
MNCV (m/s)	61.0 ± 1.5	60.5 ± 1.1	58.6 ± 1.0	50.5 ± 1.0**	52.6 ± 1.1**	51.5 ± 1.4**
SNCV (m/s)	43.8 ± 0.6	43.5 ± 0.9	42.8 ± 0.8	35.9 ± 0.9**	39.0 ± 0.7#	39.8 ± 1.0##
Thermal response latency (s)	11.7 ± 0.5	11.9 ± 0.5	12.3 ± 0.5	18.6 ± 0.8**	15.3 ± 1.2**##	14.2 ± 0.6**##
Mechanical withdrawal thresholds (g)	114 ± 4.6	100 ± 5.2	101 ± 3.9	156 ± 9.7**	110 ± 5.4##	108 ± 4.6##
Tactile response thresholds (g)	19.2 ± 1.2	19.4 ± 1.1	20.5 ± 1.0	8.6 ± 1.0**	11.0 ± 1.1**	13.9 ± 1.5**##

Data are means ± SEM. n = 8–13 per group. M1 and M2, Metanx at low and high doses, respectively. **$P < 0.01$ vs. age-matched ZDF lean rats. #$P < 0.05$ vs. untreated ZDF rats. ##$P < 0.01$ vs. untreated ZDF rats.

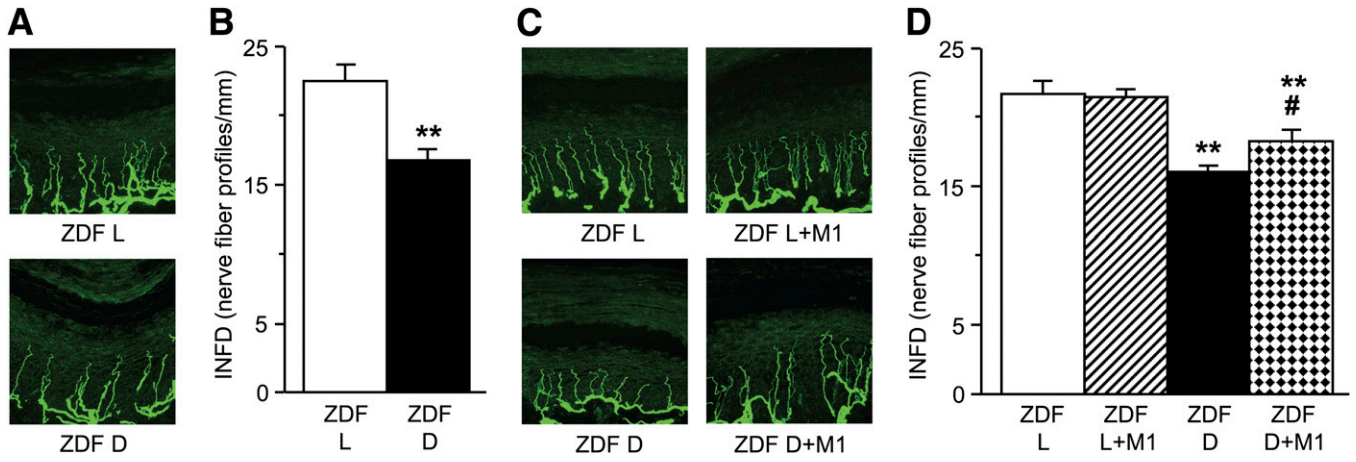

FIG. 1. Intraepidermal nerve fiber profiles in 15-week-old ZDF (ZDF D) and ZDF lean (ZDF L) rats (before Metanx treatment) (*A* and *B*) and 19-week-old ZDF D and ZDF L rats maintained with or without low-dose Metanx treatment (*C* and *D*). Representative images of intraepidermal nerve fiber profiles, magnification ×400 (*A* and *C*) and skin fiber density (*B* and *D*). M1, low-dose Metanx. Mean ± SEM, *n* = 8–10 per group. ***P* < 0.01 vs. age-matched ZDF L rats; #*P* < 0.05 vs. untreated ZDF D rats. (A high-quality digital representation of this figure is available in the online issue.)

ZDF rats compared with the ZDF lean rat group ($P < 0.01$), whereas g-ratio (axon diameter to fiber diameter) and ratio of axon diameter to myelin thickness were increased by 5 and 13% ($P < 0.05$ for both comparisons). Metanx did not affect myelin thickness, g-ratio, or ratio of axon diameter to myelin thickness in either ZDF or ZDF lean rats.

Sciatic nerve nitrate/nitrite and nitrotyrosine concentrations were 115 and 54% greater in 19-week-old ZDF rats than in ZDF lean rats ($P < 0.05$ for nitrate/nitrate and $P < 0.01$ for nitrotyrosine) (Fig. 2), consistent with the development of oxidative-nitrosative stress. Metanx treatment blunted oxidative-nitrosative stress in ZDF rats without affecting sciatic nerve nitrotyrosine or nitrate/nitrite concentrations in ZDF lean rats.

Sciatic nerve eNOS dimer level was 33.6% lower in 19-week-old ZDF rats than in ZDF lean rats ($P < 0.05$) (Fig. 3*A* and *B*). Conversely, eNOS monomer level was 34.2% higher ($P < 0.01$), indicative of diabetes-associated eNOS uncoupling. eNOS dimer and eNOS monomer levels in Metanx-treated ZDF rats were not different from those in ZDF lean rats. eNOS was localized to endothelial cells (Fig. 3*C*) but not to Schwann cells (Fig. 3*D*) or axons (Fig. 3*E*) in either ZDF or ZDF lean rats.

Sciatic nerve iNOS level was 33% higher in 19-week-old ZDF rats than in ZDF lean rats ($P < 0.01$) (Fig. 4*A* and *B*). In Metanx-treated ZDF rats, iNOS level was 22% higher than in ZDF lean rats, but the differences with either untreated ZDF or ZDF lean rats did not achieve statistical significance. iNOS was localized to endothelial (Fig. 4*C*) and Schwann cells (Fig. 4*D*) but not to axons (Fig. 4*E*) in either ZDF or ZDF lean rats.

Sciatic nerve methylglyoxal-derived AGE level was 68% higher in 19-week-old ZDF rats than in ZDF lean rats ($P < 0.01$) (Fig. 5). Methylglyoxal-derived AGE accumulation was 38% lower in Metanx-treated ZDF rats than in the untreated group ($P < 0.01$).

Sciatic nerve GSH concentrations were similar in ZDF and ZDF lean rats (0.514 ± 0.092 and 0.523 ± 0.056 μmol/g wet wt). Because of the lack of GSH depletion in untreated ZDF rats, GSH measurements in the other two groups were not performed.

DISCUSSION

In the current study in ZDF rats, an orally administered Metanx, at a body weight–based equivalent of human dose, alleviated diabetes-induced oxidative-nitrosative stress, SNCV deficit, and small sensory nerve fiber neuropathy without affecting MNCV deficit or distal tibial nerve morphometry. The efficacy of Metanx was not due to reduction of diabetic hyperglycemia. These findings have a number of implications for future experimental studies of DPN and a translational potential.

Although ~95% of human subjects with diabetes in the U.S. have type 2 diabetes, a vast majority of experimental studies related to DPN were conducted in streptozotocin

TABLE 3
Distal tibial nerve morphometric indices in ZDF and ZDF lean rats maintained with or without low-dose Metanx treatment

Group variable	ZDF lean	ZDF lean + M1	ZDF	ZDF + M1
Nerve fiber number	2,576 ± 33	2,540 ± 75	2,481 ± 43	2,500 ± 53
Nerve fiber density (fibers/mm^2)	12,225 ± 532	13,321 ± 584	12,980 ± 501	13,410 ± 296
Nerve fiber diameter (μ)	8.17 ± 0.14	8.07 ± 0.20	7.93 ± 0.15	7.77 ± 0.09
Axon diameter (μ)	5.17 ± 0.17	5.13 ± 0.18	5.25 ± 0.13	5.10 ± 0.12
Myelin thickness (μ)	1.50 ± 0.04	1.47 ± 0.04	1.34 ± 0.02**	1.34 ± 0.02**
g-Ratio (axon diameter/fiber diameter)	0.634 ± 0.011	0.636 ± 0.010	0.664 ± 0.005*	0.657 ± 0.008
Axon diameter/myelin thickness	3.65 ± 0.18	3.64 ± 0.15	4.12 ± 0.11*	4.00 ± 0.15

Data are means ± SEM. *n* = 6 rats per group. M1, low-dose Metanx. **P* < 0.05 vs. age-matched ZDF lean rats. ***P* < 0.01 vs. age-matched ZDF lean rats.

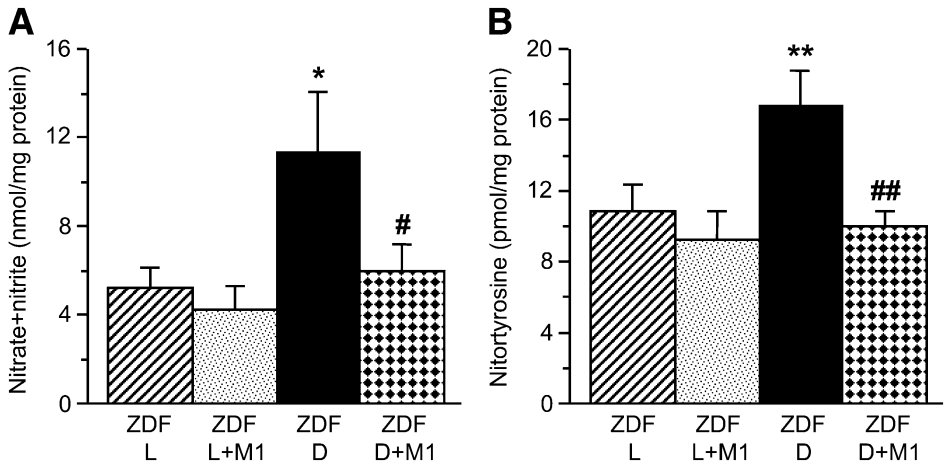

FIG. 2. ***A*** **and** ***B*****: Sciatic nerve nitrate/nitrite and nitrotyrosine concentrations in ZDF (ZDF D) and ZDF lean (ZDF L) rats maintained with or without low-dose Metanx treatment. M1, low-dose Metanx. Mean ± SEM,** n **= 7–9 per group. *P < 0.05 and **P < 0.01 vs. age-matched ZDF L rats. #P < 0.05 and ##P < 0.01 vs. untreated ZDF D rats.**

(STZ)-induced diabetic rodents. Very few reports describe DPN in animal models of type 2 diabetes, such as leptin-deficient (*ob/ob*) and leptin receptor–deficient (*db/db*) mice, BBZDR/Wor rats, and others (11,27–29). Our results, consistent with two previous studies (11,30), suggest that the ZDF rat, which displays oxidative-nitrosative stress, MNCV and SNCV deficit, thermal and mechanical hypoalgesia, small sensory nerve fiber degeneration, and a mild atrophy of large myelinated fibers, is a robust animal model for evaluating functional and morphological manifestations of insensate DPN associated with type 2 diabetes as well as potential therapeutics targeting reactive oxygen and nitrogen species formation and neutralization.

Large discrepancies between the doses of many neuropathy drug candidates tested so far in animal and human studies are well known. The doses for aldose reductase, protein kinase C, advanced glycation inhibitors, acetylcarnitine, and many other agents proven effective in animal models could not be administered to humans because of adverse side effects. Clinical trials with much lower doses of these agents showed very modest efficacy against DPN. To our knowledge, Metanx is the first oral therapeutic alleviating both functional and morphological manifestations of experimental DPN at a body weight–based equivalent of human dose. Of particular interest is the effect on INFD, a sensitive surrogate marker of small sensory nerve fiber degeneration emerging from both clinical (31,32) and experimental (25,30,33–35) studies. The ability to increase INFD in diabetic rats and mice was previously reported for a recombinant human erythropoietin (60 mg · kg^{-1} · day^{-1} i.p.) (33), insulin and insulin-like growth factor 1 (0.1 IU · day^{-1} intrathecally) (34), and, recently, a glucagon-like peptide 1 receptor agonist exendin-4 (10 nmol · kg^{-1} [41.9 mg · kg^{-1}] i.p.) (35). The advantages of orally active low-dose Metanx over the aforementioned pharmacological approaches are obvious. The high efficacy of Metanx is probably explained by the synergistic interactions of its components counteracting oxidative-nitrosative stress through restoration of eNOS coupling in vasa nervorum (L-methylfolate), neutralization of superoxide and peroxynitrite (methylcobalamin), and chelation of transition metals and abrogation of AGE formation (pyridoxal 5′-phosphate). Because superoxide, peroxynitrite, and AGEs are formed in both microvasculature and neural tissues of the peripheral nervous system (10,11,36,37), methylcobalamin and pyridoxal 5′-phosphate are likely to act on multiple cell types. Marked neurovascular synergistic interactions previously were identified between aldose reductase and ACE inhibitors (38), a protein kinase C-β inhibitor and compounds ameliorating oxidative stress and n-6 fatty acid metabolism (39), and poly(ADP-ribose) polymerase inhibitors and vasodilators (40). All these combination therapies were tested in STZ-induced diabetic rats, and none of the above-mentioned studies included INFD as end point.

Our findings provide new information on manifestations and mechanisms of oxidative-nitrosative stress in experimental type 2 DPN. Because of the extremely high rate of reaction between superoxide and NO, its product, peroxynitrite, and peroxynitrite stable footprint, nitrotyrosine, are formed in tissues under normal conditions (8). Their formation is increased in diabetes (8). We previously identified iNOS as a source of NO for excessive nitrotyrosine formation in peripheral nerve of STZ-induced diabetic mice (41). In the current study in ZDF rats, iNOS presence in endothelial and Schwann cells (i.e., two cell types that form excessive superoxide in diabetes and high glucose) and iNOS upregulation are consistent with peripheral nerve nitrotyrosine accumulation. Increased iNOS and nitrated protein levels were also identified in high glucose–exposed human Schwann cells (10,42). Peroxynitrite and nitrotyrosine ultimately decompose to nitrate/nitrite, which explains nitrate/nitrite accumulation in peripheral nerve of ZDF rats. In agreement with previous observations in BB/Wor and BBZDR/Wor rats (29), our results suggest that mechanisms of oxidative-nitrosative stress in type 1 and type 2 DPN may be different. Peripheral nerve GSH depletion, the hallmark of oxidative injury in STZ-induced diabetic rats (15,43,44), was absent in ZDF rats. ZDF rats, however, exhibited other changes leading to oxidative-nitrosative stress, such as eNOS uncoupling, iNOS overexpression, and accumulation of methylglyoxal-derived AGEs. Significant levels of methylglyoxal-derived AGEs in peripheral nerve of nondiabetic rats were also detected by others using the state-of-the-art liquid chromatography–tandem mass spectrometry method (37). A blunted nitrotyrosine and nitrate/nitrite accumulation in Metanx-treated ZDF rats is consistent with restored eNOS coupling and

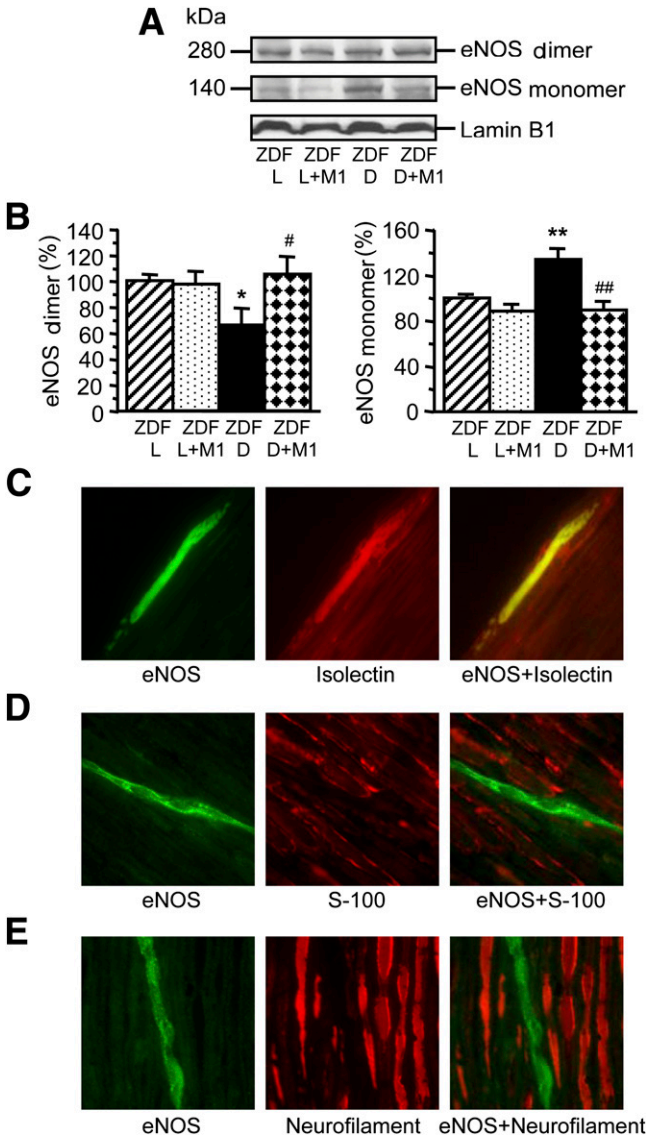

FIG. 3. Representative Western blot analysis of eNOS dimer and monomer (*A*) and their content (densitometry) (*B*) in ZDF (ZDF D) and ZDF lean (ZDF L) rats maintained with or without low-dose Metanx treatment. M1, low-dose Metanx. Mean ± SEM, n = 8 per group. *P < 0.05 and **P < 0.01 vs. age-matched ZDF L rats. #P < 0.05 and ##P < 0.01 vs. untreated ZDF D rats. *C–E*: Representative microphotographs of fluorescence immunostaining (or fluorescence staining with isolectin Alexa Fluor 594 conjugate in *C* [*center*]) of diabetic rat sciatic nerve for eNOS, vascular endothelium, and eNOS and vascular endothelium (*C*); eNOS, S-100, and eNOS and S-100 (*D*); and eNOS, Neurofilament H, and eNOS and Neurofilament H (*E*). Magnification ×630. (A high-quality digital representation of this figure is available in the online issue.)

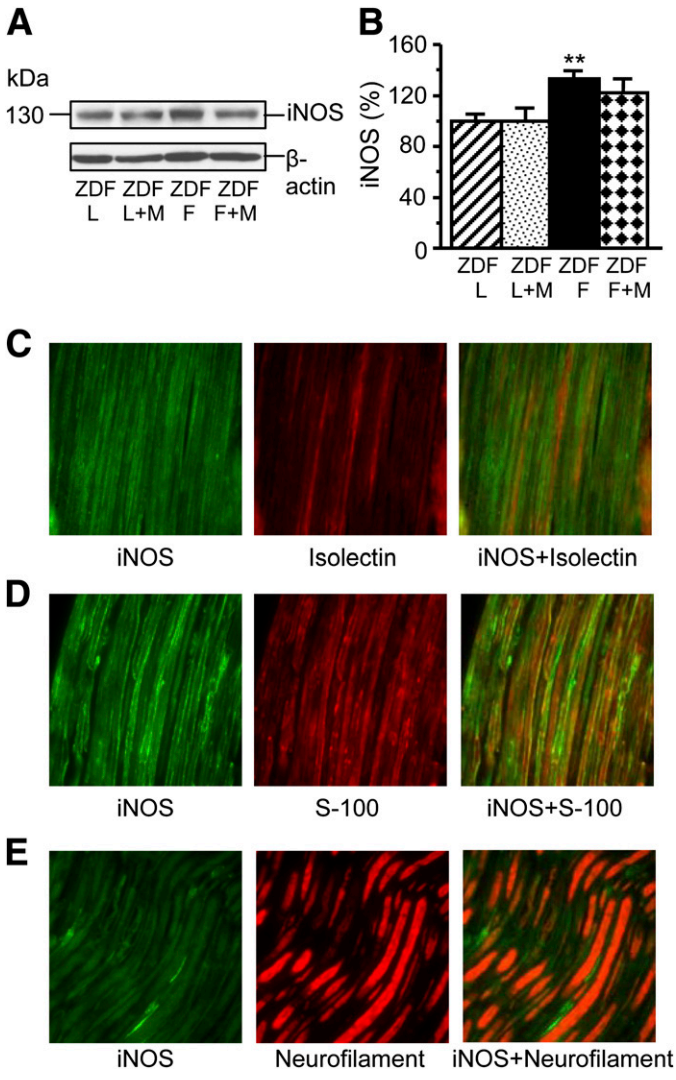

FIG. 4. Representative Western blot analysis of iNOS (*A*) and its content (densitometry) (*B*) in ZDF (ZDF D) and ZDF lean (ZDF L) rats maintained with or without low-dose Metanx treatment. M, low-dose Metanx. Mean ± SEM, n = 8–12 per group. **P < 0.01 vs. age-matched ZDF L rats. *C–E*: Representative microphotographs of fluorescence immunostaining (or fluorescence staining with isolectin Alexa Fluor 594 conjugate in *C* [*center*]) of diabetic rat sciatic nerve for iNOS, vascular endothelium, and iNOS and vascular endothelium (*C*); iNOS, S-100, and iNOS and S-100 (*D*); and iNOS, Neurofilament H, and iNOS and Neurofilament H (*E*). Magnification ×400. (A high-quality digital representation of this figure is available in the online issue.)

decreased iNOS and methylglyoxal-derived AGE levels (i.e., the changes known to reduce both superoxide and NO production).

Our findings in ZDF rats agree with and complement our previous observations in STZ-induced diabetic mice (25), suggesting differences in the pathogenetic mechanisms of large and small sensory fiber neuropathies. The aforementioned study identifies an important contribution of the enzyme of arachidonic acid metabolism, 12/15-lipoxygenase, to diabetes-induced MNCV and SNCV deficit and distal tibial nerve myelinated fiber atrophy. In contrast, the role of 12/15-lipoxygenase in small sensory nerve fiber degeneration appeared minor (25). Conversely, in the current study, Metanx alleviated sensory neuropathy without affecting MNCV or morphometric characteristics of large myelinated fibers. Note that the Metanx ingredient methylcobalamin, administered intramuscularly as a monotherapy, prevented both MNCV deficit and axonal atrophy in STZ-induced diabetic rats (18,45). Although it is difficult to compare our results with the two aforementioned methylcobalamin studies (18,45) because of the significant differences in dose, mode, and type (prevention vs. treatment) of drug administration, amenability of SNCV, but not MNCV, to experimental treatments was identified in several other studies (15,43).

The knowledge of pathogenetic mechanisms and specificities of each drug candidate obtained in experimental studies is important for selection of robust end points for clinical trials, many of which failed because of poor design and lack of sensitive measures of nerve function (46,47).

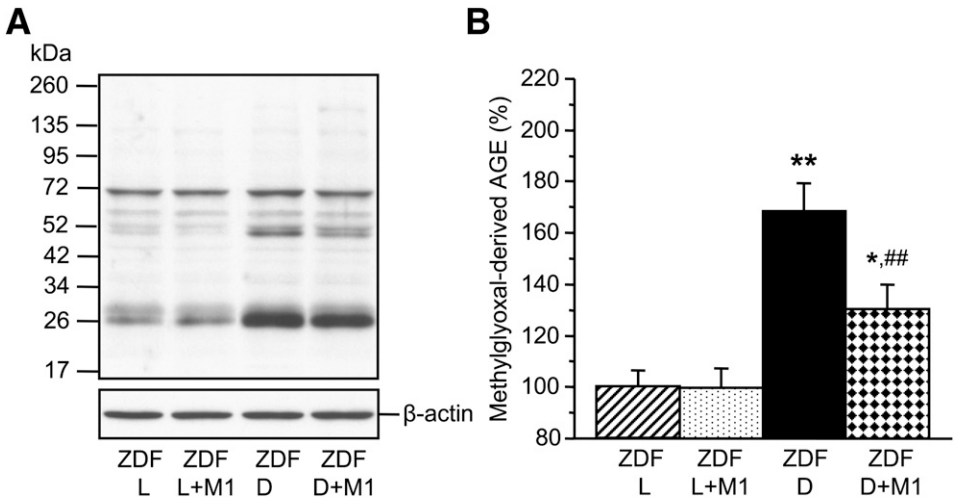

FIG. 5. Representative Western blot analysis of methylglyoxal-derived AGEs (*A*) and their content (densitometry) (*B*) in ZDF (ZDF D) and ZDF lean (ZDF L) rats maintained with or without low-dose Metanx treatment. M1, low-dose Metanx. Mean ± SEM, $n = 8$ per group. *$P < 0.05$ and **$P < 0.01$ vs. age-matched ZDF L rats. ##$P < 0.01$ vs. untreated ZDF D rats.

Although probability of discrepancy between the results of animal model studies and clinical trials is never excluded, our experimental data suggest that Metanx is more likely to exert a beneficial effect on SNCV, quantitative sensory testing measures, and INFD, rather than on MNCV and sural nerve morphometry, in human subjects with diabetes. This suggestion agrees with the results of two recent small clinical trials. In a 1-year study in 20 patients with type 2 diabetes and DPN, Metanx alleviated the loss of cutaneous sensitivity in the great toe and heel (48). In another 6-month study in 11 type 2 diabetic subjects, Metanx increased INFD at the calf (73% of subjects) and reduced frequency and intensity of paresthesias and/or dysesthesias (83% of subjects) (49).

Our results, together with current knowledge of the role for eNOS uncoupling and oxidative-nitrosative stress in the pathogenesis of several diabetes complications, provide rationale for studying Metanx on diabetic cardiovascular disease, retinopathy, and nephropathy. A beneficial effect on oxidative stress in endothelial cells and experimental diabetic vasculopathy was observed with another agent targeting eNOS, the eNOS transcription enhancer AVE3085 (50).

In conclusion, our findings and two aforementioned small clinical trials (48,49) provide rationale for further clinical studies of Metanx to determine its usefulness in improving the management of DPN. Although experimental and clinical studies of Metanx have been conducted in type 2 diabetes only, they are also relevant to type 1 diabetes because the latter is also associated with endothelial dysfunction, oxidative-nitrosative stress, and peripheral nerve dysfunction and degeneration (1,4–9).

ACKNOWLEDGMENTS

H.S., P.W., R.S., S.L., and I.G.O. were partially supported by National Institutes of Health (NIH) Grants RO1-DK-074517, RO1-DK-077141, and RO1-DK-081147 and American Diabetes Association Research Grant 7-08-RA-102. The Cell Biology and Bioimaging Core used in this work is supported in part by Centers of Biomedical Research Excellence (NIH P20-RR21945) and Clinical Nutrition Research Unit (NIH 1-P30-DK-072476) grants.

This study was supported by Pan American Laboratories (Covington, LA). No other potential conflicts of interest relevant to this article were reported.

H.S. performed all morphological measurements and double immunohistochemistry to localize eNOS to Schwann cells and axons. P.W. was responsible for animal treatment and behavioral tests. R.S. conducted all other immunohistochemical studies, Western blot analysis of iNOS, and GSH measurements. E.D. performed all morphological measurements. S.L. was responsible for MNCV, SNCV, nitrate/nitrite and nitrotyrosine enzyme-linked immunosorbent assay measurements, and Western blot analyses of eNOS dimer and monomer and methylglyoxal-derived AGE. I.G.O. wrote the manuscript. All authors participated in data discussion. I.G.O. is the guarantor of this work and, as such, had full access to all the data in the study and takes responsibility for the integrity of the data and the accuracy of the data analysis.

The authors thank Dr. Douglas E. Wright from the University of Kansas Medical Center (Kansas City, KS) for valuable recommendations regarding INFD measurements.

REFERENCES

1. Boulton AJ, Vinik AI, Arezzo JC, et al.; American Diabetes Association. Diabetic neuropathies: a statement by the American Diabetes Association. Diabetes Care 2005;28:956–962
2. Malik RA, Tesfaye S, Newrick PG, et al. Sural nerve pathology in diabetic patients with minimal but progressive neuropathy. Diabetologia 2005;48:578–585
3. Dyck PJ, Davies JL, Clark VM, et al. Modeling chronic glycemic exposure variables as correlates and predictors of microvascular complications of diabetes. Diabetes Care 2006;29:2282–2288
4. Doupis J, Lyons TE, Wu S, Gnardellis C, Dinh T, Veves A. Microvascular reactivity and inflammatory cytokines in painful and painless peripheral diabetic neuropathy. J Clin Endocrinol Metab 2009;94:2157–2163
5. Charles M, Soedamah-Muthu SS, Tesfaye S, et al.; EURODIAB Prospective Complications Study Investigators. Low peripheral nerve conduction velocities and amplitudes are strongly related to diabetic microvascular complications in type 1 diabetes: the EURODIAB Prospective Complications Study. Diabetes Care 2010;33:2648–2653
6. Obrosova IG. Diabetes and the peripheral nerve. Biochim Biophys Acta 2009;1792:931–940
7. Schmeichel AM, Schmelzer JD, Low PA. Oxidative injury and apoptosis of dorsal root ganglion neurons in chronic experimental diabetic neuropathy. Diabetes 2003;52:165–171

8. Drel VR, Lupachyk S, Shevalye H, et al. New therapeutic and biomarker discovery for peripheral diabetic neuropathy: PARP inhibitor, nitrotyrosine, and tumor necrosis factor-alpha. Endocrinology 2010;151:2547–2555
9. Lupachyk S, Shevalye H, Maksimchyk Y, Drel VR, Obrosova IG. PARP inhibition alleviates diabetes-induced systemic oxidative stress and neural tissue 4-hydroxynonenal adduct accumulation: correlation with peripheral nerve function. Free Radic Biol Med 2011;50:1400–1409
10. Obrosova IG, Drel VR, Pacher P, et al. Oxidative-nitrosative stress and poly (ADP-ribose) polymerase (PARP) activation in experimental diabetic neuropathy: the relation is revisited. Diabetes 2005;54:3435–3441
11. Oltman CL, Coppey LJ, Gellett JS, Davidson EP, Lund DD, Yorek MA. Progression of vascular and neural dysfunction in sciatic nerves of Zucker diabetic fatty and Zucker rats. Am J Physiol Endocrinol Metab 2005;289: E113–E122
12. Ziegler D, Ametov A, Barinov A, et al. Oral treatment with alpha-lipoic acid improves symptomatic diabetic polyneuropathy: the SYDNEY 2 trial. Diabetes Care 2006;29:2365–2370
13. Ziegler D, Low PA, Litchy WJ, et al. Efficacy and safety of antioxidant treatment with α-lipoic acid over 4 years in diabetic polyneuropathy: the NATHAN 1 trial. Diabetes Care 2011;34:2054–2060
14. Kishi Y, Schmelzer JD, Yao JK, et al. Alpha-lipoic acid: effect on glucose uptake, sorbitol pathway, and energy metabolism in experimental diabetic neuropathy. Diabetes 1999;48:2045–2051
15. Stevens MJ, Obrosova I, Cao X, Van Huysen C, Greene DA. Effects of DL-alpha-lipoic acid on peripheral nerve conduction, blood flow, energy metabolism, and oxidative stress in experimental diabetic neuropathy. Diabetes 2000;49:1006–1015
16. Miller AL. The methylation, neurotransmitter, and antioxidant connections between folate and depression. Altern Med Rev 2008;13:216–226
17. Antoniades C, Shirodaria C, Warrick N, et al. 5-methyltetrahydrofolate rapidly improves endothelial function and decreases superoxide production in human vessels: effects on vascular tetrahydrobiopterin availability and endothelial nitric oxide synthase coupling. Circulation 2006; 114:1193–1201
18. Mizukami H, Ogasawara S, Yamagishi S, Takahashi K, Yagihashi S. Methylcobalamin effects on diabetic neuropathy and nerve protein kinase C in rats. Eur J Clin Invest 2011;41:442–450
19. Toohey JI. Vitamin B12 and methionine synthesis: a critical review. Is nature's most beautiful cofactor misunderstood? Biofactors 2006;26:45–57
20. Moreira ES, Brasch NE, Yun J. Vitamin B12 protects against superoxide-induced cell injury in human aortic endothelial cells. Free Radic Biol Med 2011;51:876–883
21. Mukherjee R, Brasch NE. Mechanistic studies on the reaction between cob(II)alamin and peroxynitrite: evidence for a dual role for cob(II)alamin as a scavenger of peroxynitrous acid and nitrogen dioxide. Chemistry 2011; 17:11805–11812
22. Nakamura S, Li H, Adijiang A, Pischetsrieder M, Niwa T. Pyridoxal phosphate prevents progression of diabetic nephropathy. Nephrol Dial Transplant 2007;22:2165–2174
23. van Etten RW, de Koning EJ, Verhaar MC, Gaillard CA, Rabelink TJ. Impaired NO-dependent vasodilation in patients with type II (non-insulin-dependent) diabetes mellitus is restored by acute administration of folate. Diabetologia 2002;45:1004–1010
24. Yaqub BA, Siddique A, Sulimani R. Effects of methylcobalamin on diabetic neuropathy. Clin Neurol Neurosurg 1992;94:105–111
25. Obrosova IG, Stavniichuk R, Drel VR, et al. Different roles of 12/15-lipoxygenase in diabetic large and small fiber peripheral and autonomic neuropathies. Am J Pathol 2010;177:1436–1447
26. Venema RC, Ju H, Zou R, Ryan JW, Venema VJ. Subunit interactions of endothelial nitric-oxide synthase. Comparisons to the neuronal and inducible nitric-oxide synthase isoforms. J Biol Chem 1997;272:1276–1282
27. Drel VR, Mashtalir N, Ilnytska O, et al. The leptin-deficient (ob/ob) mouse: a new animal model of peripheral neuropathy of type 2 diabetes and obesity. Diabetes 2006;55:3335–3343
28. Muller KA, Ryals JM, Feldman EL, Wright DE. Abnormal muscle spindle innervation and large-fiber neuropathy in diabetic mice. Diabetes 2008;57: 1693–1701
29. Stevens MJ, Zhang W, Li F, Sima AA. C-peptide corrects endoneurial blood flow but not oxidative stress in type 1 BB/Wor rats. Am J Physiol Endocrinol Metab 2004;287:E497–E505
30. Brussee V, Guo G, Dong Y, et al. Distal degenerative sensory neuropathy in a long-term type 2 diabetes rat model. Diabetes 2008;57:1664–1673
31. Sumner CJ, Sheth S, Griffin JW, Cornblath DR, Polydefkis M. The spectrum of neuropathy in diabetes and impaired glucose tolerance. Neurology 2003; 60:108–111
32. Quattrini C, Tavakoli M, Jeziorska M, et al. Surrogate markers of small fiber damage in human diabetic neuropathy. Diabetes 2007;56:2148–2154
33. Bianchi R, Buyukakilli B, Brines M, et al. Erythropoietin both protects from and reverses experimental diabetic neuropathy. Proc Natl Acad Sci USA 2004;101:823–828
34. Toth C, Brussee V, Zochodne DW. Remote neurotrophic support of epidermal nerve fibres in experimental diabetes. Diabetologia 2006;49:1081–1088
35. Himeno T, Kamiya H, Naruse K, et al. Beneficial effects of exendin-4 on experimental polyneuropathy in diabetic mice. Diabetes 2011;60:2397–2406
36. Bierhaus A, Haslbeck KM, Humpert PM, et al. Loss of pain perception in diabetes is dependent on a receptor of the immunoglobulin superfamily. J Clin Invest 2004;114:1741–1751
37. Duran-Jimenez B, Dobler D, Moffatt S, et al. Advanced glycation end products in extracellular matrix proteins contribute to the failure of sensory nerve regeneration in diabetes. Diabetes 2009;58:2893–2903
38. Cotter MA, Mirrlees DJ, Cameron NE. Neurovascular interactions between aldose reductase and angiotensin-converting enzyme inhibition in diabetic rats. Eur J Pharmacol 2001;417:223–230
39. Cameron NE, Cotter MA. Effects of protein kinase Cbeta inhibition on neurovascular dysfunction in diabetic rats: interaction with oxidative stress and essential fatty acid dysmetabolism. Diabetes Metab Res Rev 2002;18:315–323
40. Li F, Drel VR, Szabó C, Stevens MJ, Obrosova IG. Low-dose poly(ADP-ribose) polymerase inhibitor-containing combination therapies reverse early peripheral diabetic neuropathy. Diabetes 2005;54:1514–1522
41. Vareniuk I, Pavlov IA, Obrosova IG. Inducible nitric oxide synthase gene deficiency counteracts multiple manifestations of peripheral neuropathy in a streptozotocin-induced mouse model of diabetes. Diabetologia 2008;51: 2126–2133
42. Askwith T, Zeng W, Eggo MC, Stevens MJ. Taurine reduces nitrosative stress and nitric oxide synthase expression in high glucose-exposed human Schwann cells. Exp Neurol 2012;233:154–162
43. Nagamatsu M, Nickander KK, Schmelzer JD, et al. Lipoic acid improves nerve blood flow, reduces oxidative stress, and improves distal nerve conduction in experimental diabetic neuropathy. Diabetes Care 1995;18: 1160–1167
44. Cameron NE, Cotter MA, Jack AM, Basso MD, Hohman TC. Protein kinase C effects on nerve function, perfusion, Na(+), K(+)-ATPase activity and glutathione content in diabetic rats. Diabetologia 1999;42:1120–1130
45. Yagihashi S, Tokui A, Kashiwamura H, Takagi S, Imamura K. In vivo effect of methylcobalamin on the peripheral nerve structure in streptozotocin diabetic rats. Horm Metab Res 1982;14:10–13
46. Dyck PJ, Norell JE, Tritschler H, et al. Challenges in design of multicenter trials: end points assessed longitudinally for change and monotonicity. Diabetes Care 2007;30:2619–2625
47. Boulton AJ. Whither clinical research in diabetic sensorimotor peripheral neuropathy? Problems of end point selection for clinical trials. Diabetes Care 2007;30:2752–2753
48. Walker MJ Jr, Morris LM, Cheng D. Improvement of cutaneous sensitivity in diabetic peripheral neuropathy with combination L-methylfolate, methylcobalamin, and pyridoxal 5′-phosphate. Rev Neurol Dis 2010;7:132–139
49. Jacobs AM, Cheng D. Management of diabetic small-fiber neuropathy with combination L-methylfolate, methylcobalamin, and pyridoxal 5′-phosphate. Rev Neurol Dis 2011;8:39–47
50. Cheang WS, Wong WT, Tian XY, et al. Endothelial nitric oxide synthase enhancer reduces oxidative stress and restores endothelial function in db/db mice. Cardiovasc Res 2011;92:267–275